

CIDEP Studies of Fullerene-Derived Radical Adducts

Igor V. Koptug and Artem G. Goloshevsky

International Tomography Center, Novosibirsk, Russia

Igor S. Zavarine and Nicholas J. Turro*

Department of Chemistry, Columbia University, New York, New York 10027

Paul J. Krusic

Central Research and Development, E. I. du Pont de Nemours & Company, Wilmington, Delaware 19880-0328†

Received: November 12, 1999; In Final Form: April 5, 2000

Photolyses of solutions containing organomercury compounds (HgR_2) in the presence of C_{60} fullerene have been investigated by Fourier transform time-resolved EPR (FT TR EPR) and continuous-wave EPR (CW EPR) techniques. By FT TR EPR, both electron-spin-polarized $^3\text{C}_{60}$ (A polarization) and electron-spin-polarized adducts $\cdot\text{C}_{60}\text{R}$ (E/A + E polarization) are observed. The CW EPR spectra of the $\cdot\text{C}_{60}\text{R}$ radicals under steady-state irradiation also exhibit some electron-spin polarization. The chemically induced dynamic electron polarization (CIDEP) in the FT TR EPR experiments is explained by the following series of steps. Photolysis initially causes cleavage of the organomercury compounds into radicals that add to C_{60} to form $\cdot\text{C}_{60}\text{R}$. The latter combine to form the dimers, $[\text{C}_{60}\text{R}]_2$, which are thermally stable and accumulate in the samples. In all of the reported experiments, a certain quantity of dimers is produced by photolysis before the EPR spectra are acquired. In the FT TR EPR experiments, laser excitation produces $^3\text{C}_{60}$ by excitation of C_{60} and $\cdot\text{C}_{60}\text{R}$ by photocleavage of the dimers. The observed E/A CIDEP patterns at short ($< 1 \mu\text{s}$) delays after the laser flash are proposed to be a result of the creation of polarization through the radical-pair mechanism (RPM) resulting from the interactions of two $\cdot\text{C}_{60}\text{R}$ radicals (geminate or free) formed from the photocleavage of $[\text{C}_{60}\text{R}]_2$ dimers. The additional E polarization observed at later times ($> 1 \mu\text{s}$) is proposed to result from the interaction of $^3\text{C}_{60}$ with $\cdot\text{C}_{60}\text{R}$ radicals, creating E polarization through the radical-pair-triplet mechanism (RPTM). The polarization observed in the CW EPR experiments is attributed to the maintenance of polarization through the radical lifetime because of the extremely long spin–lattice relaxation of the $\cdot\text{C}_{60}\text{R}$ radicals. The latter conclusion is consistent with the very small (50 mG) line widths of the adduct radicals. An upper limit for the bond energy of the $[\text{C}_{60}\text{R}]_2$ dimers of 226 kJ/mol is established by the observation of the CIDEP of $\cdot\text{C}_{60}\text{R}$ radicals when 532-nm excitation is employed. The role of multiple adducts in the observed FT TR EPR spectra is discussed.

Introduction

Since the discovery by Closs and co-workers¹ of the room-temperature EPR signal from the excited triplet state of the C_{60} fullerene in liquid solutions, C_{60} and its derivatives have become a subject of intense investigations by the EPR and laser flash photolysis techniques. For example, chemically induced dynamic electron polarization (CIDEP) properties of the radical anion of C_{60} ,^{2–4} of $^3\text{C}_{60}$,^{5–7} and of alkoxyfullerene radicals⁸ have been studied by FT TR EPR and CW TR EPR techniques. Alkylfullerene radicals have also been the subject of intense investigations by the conventional CW EPR technique.^{9–11} Here, we report the results of studies of the photogenerated polarized alkylfullerene radicals using CW and time-resolved FT EPR methods.

Experimental Section

Fullerene (C_{60}) was purchased from SES Research (Texas). All other materials were purchased either from Aldrich or from

Organometallics Inc. (dialkylmercury compounds) and were used without further purification. It was assumed that 1 mol of dialkylmercury compound would produce 2 mol of radicals upon photolysis. Typical dialkylmercury samples for FT TR EPR were prepared by mixing 400 μL of a 1.7 mM solution of C_{60} in benzene with 4 μL of a 0.085 M solution of dialkylmercury in *tert*-butylbenzene (1:1 radical-to- C_{60} molar ratio) or with 60 μL of a 0.017 M solution of dialkylmercury in *tert*-butylbenzene (1:3 radical-to- C_{60} molar ratio). Both types of samples gave very similar EPR spectra, except that the latter gave stronger signals. Samples were degassed and sealed in 4-mm diameter Suprasil quartz tubes. For some CW EPR experiments, samples were prepared by adding a 3- to 10-fold excess of an alkylbromide to the ca. 3 mM solution of C_{60} in toluene. In all cases, the radicals were generated by irradiation in the cavity of the EPR spectrometer with either a Lambda Physik excimer laser at 308 nm or a Nd:YAG laser at 532 nm for the time-resolved work or by broadband xenon lamp light filtered by a glass water filter ($\lambda > 310 \text{ nm}$) for the CW experiments. Our FT TR EPR setups have been previously described in detail.¹² The lines in the FT

† Du Pont Contribution No. 7986.

EPR spectra of the radicals were narrow, so it was essential to zero fill the FID's up to 256 K or more before Fourier transforming them. FT EPR spectra were simulated using homemade simulation programs. Simulations of the CW EPR spectra were performed using a Bruker WinEPR Symphonia software package. CW EPR spectra were acquired on a Bruker ESP 300 spectrometer. Very low modulation amplitudes (typically 0.05 G) at 50 or 100 kHz modulation frequency at low microwave powers (<200 μ W) were used for the CW EPR experiments because of the very narrow lines encountered.

Results and Discussion

Photochemistry of Dialkylmercury Compounds. The photochemistry of the dialkylmercury compounds investigated in the presence of C_{60} is summarized in eqs 1–4, with diisopropylmercury as a typical starting material. Initial UV light irradiation of the mixture of diisopropylmercury and C_{60} in benzene leads to the photolysis of the dialkylmercury compound and the formation of two isopropyl radicals, eq 1. The addition of each of these radicals to the fullerene (eq 2) is followed by a subsequent recombination of two alkylfullerene molecules to form the dimer $[(CH_3)_2CH-C_{60}]_2$, eq 3. (We note here that multiple addition of the radicals to form $^*C_{60}-R_n$ is possible, and we will discuss this issue later.) We will show that photocleavage of the dimers (eq 4) can be achieved by photolysis at 532 nm to form two $^*C_{60}-CH(CH_3)_2$ adducts and that this step leads to polarized radicals. The dimers thus formed (eq 4) are quite stable thermally and could be photolyzed literally years after they are created by an initial photolysis.



CIDEP from Photolysis of Diisopropylmercury. Isopropylfullerene Radicals. CIDEP properties of the alkylfullerene radicals are exemplified by the EPR spectra of the isopropylfullerene radical, $(CH_3)_2CH-C_{60}^*$, in Figure 1. EPR data for this and other radicals are summarized in Table 1.

A typical FT TR EPR spectrum obtained by photolysis of a diisopropylmercury sample at 308 nm is shown in Figure 1a, appearing with a net emission. The deadtime problem and the associated uncertainty in the phase of the signal in the FT EPR experiment complicate the interpretation of the phase of the FT EPR signal. However, the phase of the FT EPR signal can be verified in the following way. An FT EPR spectrum of a stable nitroxide radical is detected first, with one of the hyperfine components of the spectrum tuned exactly in resonance with the microwave field. A frequency-independent phase correction is applied to yield a purely absorptive line, as no ambiguity exists regarding the EPR spectrum phase of the thermally polarized species. Next, the spectra of short-lived radicals are detected under the same conditions, and the line in question is brought into exact resonance with the microwave field by adjusting only the value of the magnetic field. A frequency-independent phase correction identical to that used for the nitroxide radical yields the correct phase of the line considered. The procedure is repeated for other hyperfine lines as necessary. Application of this procedure allows us to unambiguously conclude that net E + multiplet E/A polarization is observed.

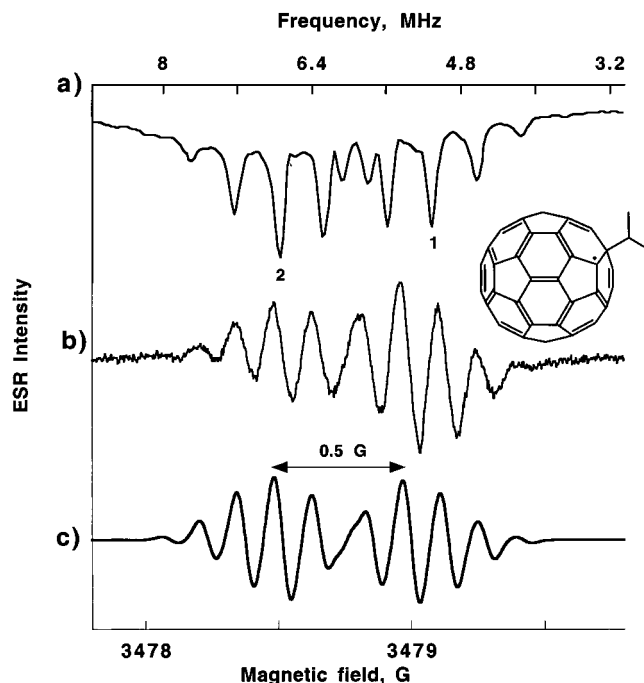


Figure 1. (a) FT TR EPR spectrum from irradiation of the mixture of diisopropylmercury and C_{60} 32 μ s after the laser pulse, (b) first-derivative CW EPR spectrum from the same sample, and (c) simulation of the CW EPR spectrum. All parameters are given in Table 1.

TABLE 1: Hyperfine Coupling Constants for the R- C_{60}^* Radicals Produced by Photolysis of the Corresponding Dimers

radical	HFCC from FT TR EPR, G	HFCC from CW EPR, G ^a
CH ₃	3H = 0.03 \pm 0.01	3H = 0.034 ^b
CH ₃ CH ₂	2H = 0.27, 3H = 0.114	2H = 0.27, 3H = 0.125
(CH ₃) ₂ CH	1H = 0.472, 6H = 0.137	1H = 0.485, 6H = 0.14
(CH ₃) ₃ C	^c	9H = 0.17 ^d
C ₆ H ₅ CH ₂	2H = 0.416, 2H = 0.184	2H = 0.41, 2H = 0.18 ^e

^a At ca. 40 °C; \pm 0.005 G except see footnote b; obtained by simulation (Bruker's Symphonia). ^b \pm 0.01 G, line width 0.03 G. Better simulation is achieved assuming nonequivalent hydrogens: 1H = 0.055, 2H = 0.029 G, line width 0.03 G, because even the methyl substituent in $CH_3-C_{60}^*$ experiences a slight barrier hindering rotation around its symmetry axis.¹³ ^c The spectrum at room temperature was not a binomial 10-line pattern as a result of selective line broadening due to hindered internal rotation of the *tert*-butyl group.¹³ ^d Fast-exchange limit HFCC. ^e Photolysis of benzyl chloride and C_{60} in toluene.

The same procedure gives net absorption (A) for the C_{60} triplet that is also observed in all of the EPR spectra detected (shown only in Figure 4, vide infra). An independent verification of the polarization signs comes from the CW TR EPR experiment, in which the absorptive line of the C_{60} triplet and a poorly resolved emissive multiplet are observed. Although signals were also observed by CW TR EPR, the signal/noise ratio was much lower, and the hyperfine pattern was less well resolved. As a result, in this report, we will only consider the time-resolved results obtained employing the FT method.

The corresponding CW EPR spectrum obtained by irradiation of the same sample of diisopropylmercury by the broadband xenon lamp is shown in Figure 1b. In the absence of light, no EPR signal is observed in the FT TR EPR experiment. (However, only for this sample did we also observe a broad absorptive line in the CW ESR in the absence of light, and we assign this broad line to the low concentration of stable radical products of the addition of many isopropyl radicals to the C_{60} unit.) The FT TR EPR and CW EPR spectra of Figure 1 are

assigned to the isopropylfullerene radical, because the hyperfine parameters for this adduct match those reported in the literature.¹³ The simulations of the CW spectra of all radicals described here give the correct line positions, although they do not account for line-width variations and intensity redistributions due to polarization effects.

CIDEP Contribution to CW EPR. The high-field portion of the CW EPR spectrum in Figure 1b is noticeably more intense than the lower-field portion, because the emission and absorption contributions are different for the two halves of the spectrum. The intensity is reduced in the downfield portion of the spectrum by an emissive component and is increased in the upfield portion of the spectrum by an absorptive component. The same asymmetry (to a lesser degree, however) is observed in Figure 3 of ref 13 (see below). We propose that the isopropylfullerene radical is polarized even under steady-state irradiation and, thereby, changes the appearance of the CW EPR spectrum. Indeed, the rare case of an observation of polarization in the CW EPR spectra was clearly established for the $\cdot\text{C}_{60}\text{H}$, $\text{OPF}_2\text{C}_{60}\cdot$, and $(\text{CH}_3)_3\text{COPF}_2\text{C}_{60}\cdot$ radicals.^{14,15} In the case of $\cdot\text{C}_{60}\text{H}$, the low-field portion of the doublet is in emission, and the high-field line of the doublet is in absorption. In the case of phosphorus-containing radicals, the spectrum also exhibits a doublet due to a large phosphorus splitting (with each line of the doublet additionally split by ^{19}F), with all of the low-field lines of this doublet in emission and the high-field lines in absorption. Small CIDEP contributions have been invoked to explain the deviations of the individual line intensities in the CW EPR spectra of the alkoxyfullerene radicals $\text{CH}_3\text{CH}_2\text{O}-\text{C}_{60}\cdot$, $(\text{CH}_3)_2\text{CHO}-\text{C}_{60}\cdot$, and $(\text{CH}_3)_3\text{CO}-\text{C}_{60}\cdot$ from those predicted by a binomial formula.⁸ For these radicals, the upfield lines appear to be more intense than the corresponding downfield lines, which are reduced in height by partial emission (negative contribution). This is exactly what is observed in the CW EPR spectrum of the alkylfullerene radicals. CIDEP kinetics data (see below) are in agreement with these conclusions. The observation that polarization is still observable at hundreds of microseconds in FT TR EPR (discussed below) suggests that the T_1 relaxation times of the fullerene adduct radicals are sufficiently long to allow observation of CIDEP in the CW EPR spectra.

The photogenerated isopropylfullerene radicals exhibit, by FT TR EPR analysis, multiplet E/A and net E polarization. Figure 1a clearly displays a departure of the relative intensities from the binomial distribution depending on the nuclear quantum number, M_i , for the two types of hydrogens (^1H , $M_i = \pm 1/2$, and ^6H , $M_i = \pm 3, 2, 1, 0$). The upfield septet is slightly stronger than the downfield septet ($\pm 1/2$), and within each septet, the outer lines are weaker than the inner lines. Such behavior can be explained by a contribution of the form $E_{ij} \times M_i \times M_j$ to both spin-lattice and spin-spin relaxation rates of the radicals, with M_i and M_j being the nuclear quantum numbers for the two groups (^1H and ^6H) of hydrogens. This implies that the anisotropy of the hyperfine coupling with the $\text{CH}_3-\text{C}(\cdot\text{H}^*)-\text{CH}_3$ hydrogen is much larger than that for the methyl.

CIDEP from Photolysis of Diethylmercury. Ethyl Fullerene Radical.

The FT TR EPR (Figure 2a) and CW EPR (Figure 2b) spectra of the radicals were generated by photolysis of the mixture of diethylmercury and C_{60} in benzene. Just like the isopropylfullerene radical, ethylfullerene exhibits multiplet E/A polarization soon after the laser pulse (Figure 2a). This polarization changes with time to a net E polarization lasting a few hundred microseconds. Simulation of the CW EPR spectrum (Figure 2c) provides the following values for the hyperfine couplings for

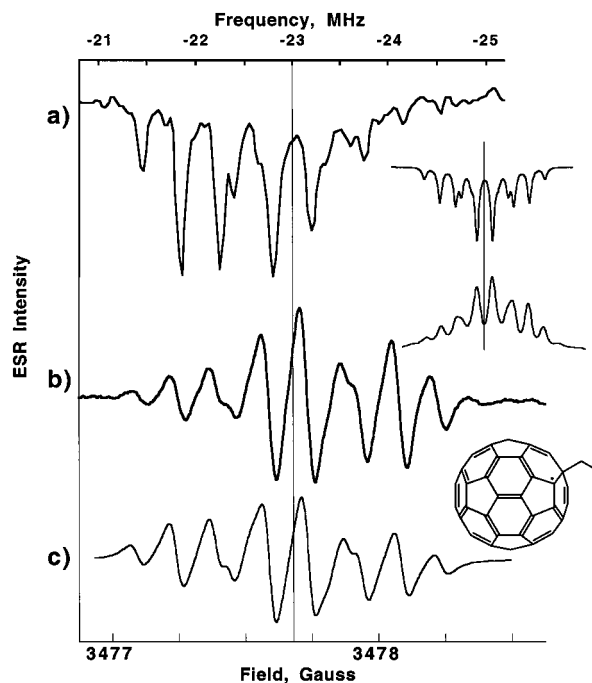


Figure 2. (a) FT TR EPR spectrum from irradiation of the solution of diethylmercury and C_{60} 64 μs after the laser pulse. The nonpolarized spectrum is expected to be symmetric with respect to the solid vertical line; the insert shows the integrated (FT) simulation of the nonpolarized spectrum. (b) First-derivative CW EPR spectrum from the same sample; the insert shows the integrated CW EPR spectrum. The nonpolarized integrated spectrum is expected to be symmetric with respect to the solid vertical line. (c) Simulation of the nonpolarized derivative (CW EPR) spectrum.

this sample: $A_{2\text{H}} = 0.27$ G and $A_{3\text{H}} = 0.125$ G. These values are very close to those reported previously at 360 K ($A_{2\text{H}} = 0.28$ G and $A_{3\text{H}} = 0.12$ G).¹³ The high-field portion of the spectrum (to the right from the line in the insert in Figure 2b) is somewhat more intense than the low-field portion (cf. Figure 3 in ref 13). Careful examination of the FT TR EPR spectrum in Figure 2a reveals that the downfield quartet corresponding to $M_i = 1$ (or -1) has the strongest intensity, followed by the quartet corresponding to $M_i = 0$ with an intermediate intensity. The third, upfield quartet, corresponding to $M_i = -1$ (or $+1$), is so weak that one can hardly see it because it is masked by a significant absorption contribution. Of all of the radicals studied here, ethylfullerene appears to exhibit the strongest amount of polarization in both the CW and the FT TR EPR spectra.

CIDEP from the Photolysis of Dibenzylmercury. The Benzyl Fullerene Radical. Figure 3a shows the FT TR EPR spectrum of the photogenerated benzylfullerene radical produced by irradiation of the mixture of dibenzylmercury and C_{60} in benzene. Figure 3b shows the corresponding CW EPR spectrum produced by irradiation of the mixture of benzyl chloride and C_{60} in toluene. Simulation of the CW EPR spectrum (Figure 3c) affords the hyperfine couplings for this radical ($A_{2\text{H}} = 0.41$ G and $A_{2\text{H}} = 0.18$ G) obtained at 313 K, which compare well with those at 350 K.¹⁰ Previous work using partially deuterated substrates has established that 0.42 G coupling belongs to benzylic protons and that the second coupling of 0.19 G belongs to meta hydrogens of the phenyl ring.¹⁶ Interestingly, both FT and CW EPR spectra show a relatively weak multiplet CIDEP effect, as they compare nicely with the simulation based on binomial intensities.

As for the results shown in Figures 1–3, FT TR EPR and CW EPR spectra were also obtained for R = methyl and *tert*-butyl radicals from photolysis of the corresponding alkyl

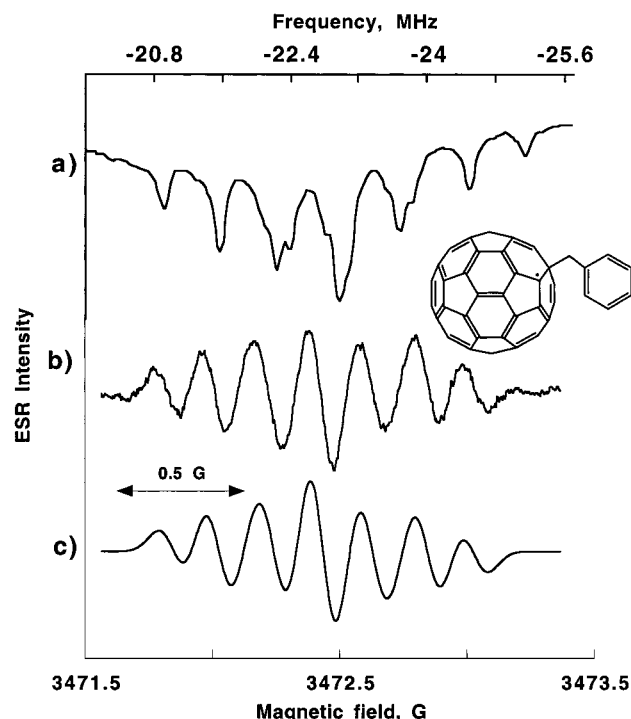


Figure 3. (a) FT TR EPR spectrum from irradiation of the solution of dibenzylmercury and C_{60} 16 μ s after the laser pulse, (b) first-derivative CW EPR spectrum from the irradiation of the mixture of benzyl chloride and C_{60} , and (c) simulation of the CW EPR spectrum.

mercury precursors. The results of the FT and CW spectral analyses are summarized in Table 1. The methylfullerene radical has a particularly weak (0.034 ± 0.01 G) hyperfine interaction due to hydrogen atoms, as was reported previously.^{16,17}

Estimation of the Bond Strength of Fullerene Dimers. The photolyses described above were conducted with 308 nm excitation, resulting in photocleavage of the dialkylmercury molecules and in situ formation of the fullerene dimers (eq 3). As mentioned above, essentially the same spectra as those shown in Figures 1 and 2 can be produced using 532 nm Nd:YAG laser excitation (FT TR EPR) or filtered (CW, $\lambda > 520$ nm) output of the xenon lamp. Because C_{60} absorbs in the visible region, it is reasonable to assume that dimers formed in situ (eq 3) would also absorb in the visible part of the spectrum. Because the dialkyl mercury compounds do not absorb significantly in the visible region, we propose that the fullerene dimer is photocleaved into fullerene radicals (eq 4) by this long-wavelength excitation and that these radicals are responsible for the observed polarization. From the energy output of 532 nm photons, we can put an upper limit on the strength of the carbon-carbon bond in $[CH_3CH_2C_{60}]_2$ {and $[(CH_3)_2CHC_{60}]_2$ } that binds the two fullerene units at 532 nm or 226 kJ/mol. This value should be compared with the value of 369 kJ/mol (ethane) for sp^3 -hybridized carbons.¹⁸ The related $[C_{60}BH_2-NMe_3]_2$ dimer cleaves under 620–680 nm irradiation, placing an even smaller upper limit on the strength of the C–C bond in that dimer (184 kJ/mol).¹¹ The enthalpy of the dimerization reaction between two isopropylfullerene radicals and of the corresponding dimer (eq 3) was measured at 149 kJ/mol.¹⁰ In the case of the significantly larger radicals $\cdot C_{60}P(O)(OR)_2$ and $\cdot C_{60}(\text{adamantanyl})$, this enthalpy of dimerization could be even lower, i.e., on the order of 54.5 and 90.5 kJ/mol, respectively.^{10,19}

Origins of CIDEP from Photolysis. Because the same CIDEP is observed by excitation at 308 or 532 nm, we propose that the observed polarization results from excitation of C_{60} and the fullerene dimers resulting from dimerization of alkyl

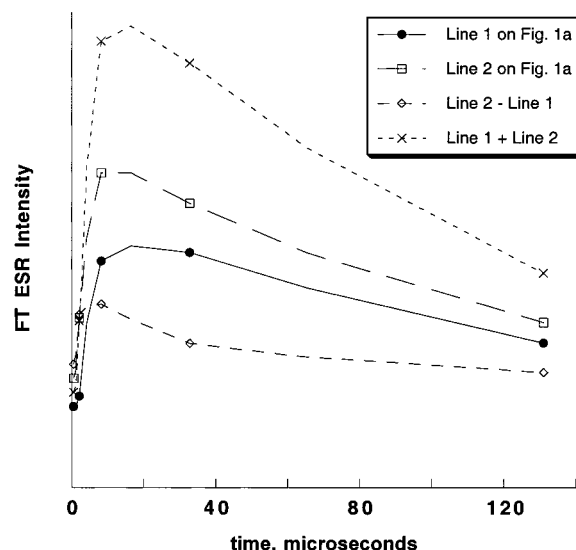
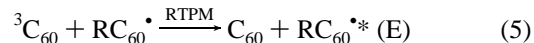


Figure 4. Time evolution of the FT TR EPR spectrum from irradiation of the mixture of diisopropylmercury and C_{60} . All features of ${}^3C_{60}$ and $C_{60}CH(CH_3)_2$ are shown in absorption, for clarity of presentation. The actual phase of ${}^3C_{60}$ is A and of the $\cdot C_{60}CH(CH_3)_2$ is E (see Figure 1).

fullerene radicals (eq 3). Consequently, we seek to explain the CIDEP observed in Figures 1–3 in terms of the interactions of paramagnetic species generated from excitation of C_{60} and the fullerene dimers formed in situ (eq 3). The photoexcitation of C_{60} produces ${}^3C_{60}$, and photoexcitation of fullerene dimers produces $\cdot C_{60}R$ radicals. We propose that the E polarization results from interactions of ${}^3C_{60}$ and $\cdot C_{60}R$ by the radical-pair-triplet mechanism (RPTM), as shown in eq 5



where $RC_{60}\cdot^*(E)$ represents an emissively polarized alkylfullerene radical. We propose that the origin of the multiplet E/A CIDEP in the CW EPR is a radical-pair mechanism (RPM) involving interactions between two $\cdot C_{60}R$ radicals, as in eq 6.



CIDEP is not commonly observed in CW EPR spectra. That CIDEP is observed in the CW EPR spectra reported here is probably due to a very long T_1 time of the $\cdot C_{60}R$ radicals (see below). If the relaxation time is longer than the lifetime of the radical polarized by RPM or RPTM, each radical would be polarized during the entire radical lifetime.

We will examine the observed polarization in the FT TR EPR spectra in terms of net E and multiplet E/A patterns. We have also considered all other established common mechanisms of CIDEP {the triplet mechanism, two types of the S–T₁ mechanism [hyperfine-induced (HFI) and spin-rotation-induced], the radical-pair mechanism (S–T₀), and the radical-triplet-pair mechanism (RTPM)} in interpreting the observed FT TR EPR spectra with the following results:

(1) The triplet mechanism (TM) predicts net E polarization (assuming that the $RC_{60}-C_{60}R$ dimer cleaves from its triplet state), but experimentally, the CIDEP maximizes at ca. 10 μ s delays (vide infra, Figure 5), which is far too long for any reasonable triplet relaxation time. Also, TM does not predict the multiplet (E/A) CIDEP that is observed.

(2) The hyperfine-induced S–T₁ mechanism could produce a mixed (net + multiplet) pattern, but would require a rather large average exchange interaction (on the order of the external

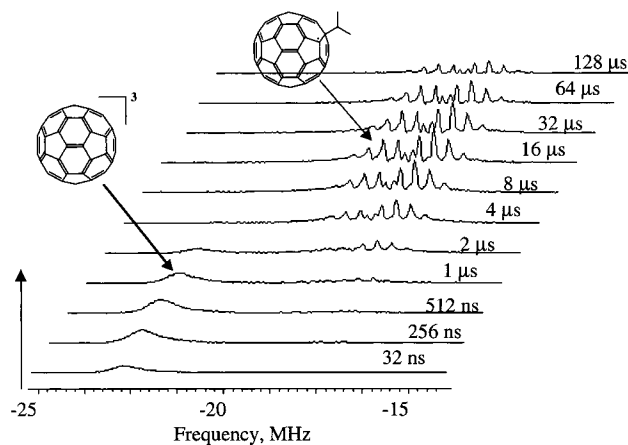


Figure 5. Evolution of the FT TR EPR intensity for the spectra shown in Figure 1a.

field, 3500 G), which is unusual and unexpected for nonviscous solvents. In addition, the rates of $T_{-} \rightarrow S$ transitions are expected to be extremely low because of the very small values of hyperfine coupling constants (HFCC's) in these radicals.

(3) The spin-rotation-induced $S-T_{-}$ mechanism could give pure net emission (hyperfine-component-independent), but this mechanism would also require a large average exchange in the radical pair. Also, a substantial spin-rotational interaction could cause rapid spin-lattice and spin-spin relaxation of the ${}^{\bullet}C_{60}R$ radical. This possibility is rendered unlikely because of the very narrow lines (0.15 MHz, or ca. 0.05 G) observed. In addition, a strong spin-rotation usually goes hand in hand with a large deviation of the g -factor from that of a free electron, which is clearly not the case in the observed spectra ($g = 2.00215$).¹⁰

(4) The pure radical-pair mechanism (RPM) in the geminate pair could give multiplet E/A polarization, but not net E (the RP is symmetric, and the g -factors are equal).

Although no single mechanism is consistent with the results, a combination of the RPTM (eq 5) and the RPM (eq 6) provides a reasonable framework for interpreting the results.

We suggest that the net emission, which grows in on the microsecond time scale, is the result of the RPTM due to the interaction of a ${}^{\bullet}C_{60}-R$ radical with the triplet state of C_{60} . The multiplet E/A effect superimposed on top of the net emission can originate (i) from the same RPTM via hyperfine interactions, and/or (ii) in F-pairs of two identical ${}^{\bullet}C_{60}-R$ radicals, and (iii) from RPM in the primary triplet pair. The contribution of F-pairs (in contrast to geminate pairs) depends on the reactivity of radicals toward dimerization, because F-pairs have random spin configurations and recombination is required to remove singlet pairs so that the remaining triplet pairs can produce CIDEP. The reason no CIDEP is observed for stable radicals in solution is that they do not recombine. Similarly, in the RPTM, the doublet pairs undergo partial quenching, i.e. quenching of the triplets by doublet radicals, which provides the excess of quartet pairs and produces polarization. It is possible that the contribution of the F-pairs to polarization is dependent on the substituent and appears to be larger for $R = \text{ethyl}$ than for $R = \text{isopropyl}$. Because the lifetime of the radicals is long, the recombination into dimers is very inefficient, and any increase in the recombination rate (e.g., because of steric factors) should lead to a larger multiplet CIDEP in F-pairs. One additional argument to support the RPTM is the observation of an E + E/A pattern for a nitroxide, when the solution of $C_{60} + \text{nitroxide}$ is photolyzed.²⁰

The E/A multiplet effect observed at very early delays most likely comes from the geminate pair, which should be produced

upon the cleavage of a triplet precursor, because a singlet precursor would yield a singlet pair and the multiplet effect would be A/E. If a triplet is involved, there could be another contribution to the net emission coming from the RTPM interaction of the ${}^{\bullet}C_{60}-R$ radical with the dimer triplet. The way to overcome this ambiguity would be to study the kinetics of formation of ${}^{\bullet}C_{60}-R$ radicals by laser flash photolysis. If the lifetime of the radical precursor were much shorter than several microseconds, we would be able to exclude this mechanism of CIDEP. Unfortunately, the low radical yield precludes an analysis by flash photolysis. (NMR experiments suggest that there are more than four products in this photoreaction.)

CIDEP Simulations. Interestingly, the experimental CIDEP pattern for the C_{60} -isopropyl radical can be reproduced reasonably well if CIDEP is calculated for a pair of radicals with the fictitious $S = 1/2$ radical with no magnetic nuclei and with the g -factor equal to that of the C_{60} triplet, using the conventional $Q^{1/2}$ intensity dependence used for normal radical pairs.²¹ This $Q^{1/2}$ calculation was shown to be justified for a pair involving a C_{60} triplet.²¹ Greater agreement can be achieved if one takes into account the different line widths for the different hyperfine components. When C_{60} triplets are involved, it is likely that the mixing of states is caused not by the dipolar interaction in the molecular triplet (as ZFS parameters D and E are relatively small for the C_{60} triplet), but rather by the HFC and Δg interactions.²⁰

CIDEP Kinetics. The occurrence of a mix of the RPTM and the RPM as the origin of the observed polarization is consistent with the CIDEP kinetics. From Figure 4, at the earliest times, the C_{60} triplet is clearly evident at high fields (low frequencies). At about 1 μs after laser excitation, the development of the E + E/A CIDEP is apparent because of the combination of RPTM and RPM. (It should be noted that the phases of the spectra shown in Figure 4 are shown as absorption for clarity of presentation of the stack diagram; however, the C_{60} triplet is A and the ${}^{\bullet}C_{60}-R$ is E, cf. Figure 1.)

Perhaps the most unusual feature of the photogenerated fullerene radicals is the very sluggish kinetics of their polarization rise and decay (Figure 4). Polarization generated through conventional CIDEP mechanisms typically rises very quickly (few hundred nanoseconds) and decays completely within 10 μs or less. However, the time evolution of the CIDEP pattern of different hyperfine lines of the isopropylfullerene radical lasts for a few hundreds of microseconds, Figure 5. Kinetics of the net and multiplet effects have maxima at close (but different) delays (Figure 5), which agrees with two different mechanisms (RPTM and RPM) contributing to the overall pattern. Assuming an exponential decay of polarization, an apparent lifetime could be estimated at ca. 70 μs . The maximum of net E at ca. 10 μs is in agreement with the lifetime of the C_{60} triplet (49 μs in benzene solution at room temperature²²), reduced significantly because of its quenching by ${}^{\bullet}C_{60}R$ radicals (which is essential for RPTM). The disappearance of the signal is probably due to both spin-lattice relaxation and recombination of the ${}^{\bullet}C_{60}-R$ radicals to yield the dimers.

Multiple Adducts. It is known that, in addition to the monoadduct radicals (${}^{\bullet}C_{60}R$), multiple adducts (${}^{\bullet}C_{60}R_n$) are also formed upon addition of radicals R to C_{60} .⁹ In fact, our results do not distinguish between ${}^{\bullet}C_{60}R$ and ${}^{\bullet}C_{60}R_n$ radicals; if other R groups are attached to C_{60} far from the radical center, their contribution to the HFC pattern will be vanishingly small. It is known in the literature that for $R = \text{benzyl}$, multiple addition occurs regioselectively.⁹ Along with the monoadduct, the allyl

radical ($\bullet\text{C}_{60}\text{R}_3$) and then the cyclopentadienyl radical ($\bullet\text{C}_{60}\text{R}_5$) are formed. (Further addition of benzyls is not regioselective.) All added benzyls add small but nonvanishing HFCC's to the multiple adduct, and a broad EPR line is expected. In our experiments, we see a strong broad emissive line (see Figure 3a) underlying the sharp lines of the monoadduct, which we assign to polarized multiple adducts. This observation is in agreement with the work of Fischer and co-workers who observed triple adducts (EPR signal 1.5 G wide, $g = 2.00245$) at high conversion.²³ Our dibenzylmercury/ C_{60} samples did not display any measurable CW EPR spectra, so we cannot confirm this conclusion independently. Photolysis of mixtures of benzyl chloride with C_{60} does produce a benzylfullerene radical pattern superimposed on a ca. 2 G broad (and weak) EPR line.

The multiple radical adducts are polarized, providing support for the RTPM for polarization of the monoadducts as follows. Because the multiple radical adducts are stable toward dimerization, they are persistent and can achieve significant concentrations, capable of interacting with triplets and becoming emissively polarized by the RTPM. Thus, the observation of a strong broad emission line assigned to the multiple adducts provides support for the RTPM of monoadducts.

Conclusions

The photolysis of solutions of C_{60} and alkylmercury compounds (eqs 1–4) produces fullerene adduct radicals, $\bullet\text{C}_{60}\text{R}$, which dimerize to yield thermally stable, but photochemically active, dimers $[\text{RC}_{60}]_2$. The photolysis of solutions containing the dimers and C_{60} result in the CIDEP reported in Figures 1–4. The E/A + E CIDEP observed in the FT TR EPR experiments results from a combination of polarization due to the RTPM resulting from interactions of $\bullet\text{C}_{60}\text{R}$ radicals and $^3\text{C}_{60}$ (E, eq 5) and to the RPM resulting from interactions of $\bullet\text{C}_{60}\text{R}$ radicals (E/A, eq 6). The CIDEP observed in the CW EPR experiments results from the long spin–lattice relaxation times of $\bullet\text{C}_{60}\text{R}$ radicals. Ethylfullerene and isopropylfullerene radicals exhibit the strongest CIDEP contribution to the CW EPR spectra and give the strongest FT TR EPR signals. FT TR EPR results probably overestimate the contribution of the monoadducts $\bullet\text{C}_{60}\text{R}$ relative to that of the multiple adducts ($\bullet\text{C}_{60}\text{R}_3$, $\bullet\text{C}_{60}\text{R}_5$, etc.). In the CW TR EPR spectra, the sharp lines of $\bullet\text{C}_{60}\text{R}$ are readily observed at low conversions only, especially for $\text{R} = \text{PhCH}_2$. For prolonged photolysis, the spectra are dominated by the broad structureless emissive signals, tentatively assigned to multiple adducts $\bullet\text{C}_{60}\text{R}_n$ ($n = 3, 5$, etc.). The unusually sluggish kinetics of the polarization's rise and subsequent decay in the FT TR EPR spectra is consistent with the CW EPR spectra also being polarized, as both are due to slow bimolecular processes that lead to polarization. The alkylfullerene dimers have very weak

carbon–carbon bond energies {less than 226 kJ/mol for $[\text{CH}_3\text{—CH}_2\text{C}_{60}]_2$ and $[(\text{CH}_3)_2\text{CHC}_{60}]_2$ }. These dimers can be photolyzed and cleaved into alkylfullerene radicals by excitation at 532 nm.

Acknowledgment. The authors thank Prof. Hans van Willigen (University of Massachusetts at Boston) for helpful discussions. Generous support from the National Science Foundation (Grant CHE98-12676) is gratefully acknowledged. I.V.K. thanks A. Okotrub (Institute of Inorganic Chemistry of the Siberian Branch of the Russian Academy Sciences) for a supply of C_{60} and the Siberian Branch of RAS and RFBR (Grant 99-03-33488) for financial support.

References and Notes

- (1) Closs, G. L.; Gautam, P.; Zhang, D.; Krusic, P. J.; Hill, S. A.; Wasserman, E. *J. Phys. Chem.* **1992**, *96*, 5228.
- (2) Ruebsam, M.; Dinse, K. P.; Plueschau, M.; Fink, J.; Kraetschmer, W.; Fostropoulos, K.; Taliani, C. *J. Am. Chem. Soc.* **1993**, *114*, 10059–10061.
- (3) Yang, C. C.; Hwang, K. C. *J. Am. Chem. Soc.* **1996**, *118*, 4693–4698.
- (4) Bennati, M.; Grupp, A.; Bauerle, P.; Mehring, M. *Chem. Phys.* **1994**, *185*, 221–227.
- (5) Regev, A.; Gamliel, D.; Meiklyar, V.; Michaeli, S.; Levanon, H. *J. Phys. Chem.* **1993**, *97*, 3671–3679.
- (6) Michaeli, S.; Meiklyar, V.; Schulz, M.; Mobius, K.; Levanon, H. *J. Phys. Chem.* **1994**, *98*, 7444–7447.
- (7) Steren, C.; Levstein, P. R.; van Willigen, H.; Linschitz, H.; Biczok, L. *Chem. Phys. Lett.* **1993**, *204*, 23–28.
- (8) Borghi, R.; Lunazzi, L.; Placucci, G.; Cerioni, G.; Plumitallo, A. *J. Org. Chem.* **1996**, *61*, 3327–3331.
- (9) Krusic, P. J.; Wasserman, E.; Keizer, P. N.; Morton, J. R.; Preston, K. F. *Science* **1991**, *254*, 1183–1185.
- (10) Morton, J. R.; Preston, K. F.; Krusic, P. J.; Wasserman, E. *J. Chem. Soc., Perkin Trans. 2* **1992**, 1425–1429.
- (11) Tumanski, B. L.; Bashilov, V. V.; Solodnikov, S. P.; Bubnov, N. N.; Sokolov, V. I.; Kampel, V. T.; Warshavsky, A. *Russ. Chem. Bull.* **1994**, *43*, 624–626.
- (12) Koptuyg, I. V.; Bossmann, S. H.; Turro, N. J. *J. Am. Chem. Soc.* **1996**, *118*, 1435.
- (13) Krusic, P. J.; Roe, D. C.; Johnston, E.; Morton, J. R.; Preston, K. F. *J. Phys. Chem.* **1993**, *97*, 1736–1738.
- (14) Morton, J. R.; Preston, K. F.; Krusic, P. J.; Knight, L. B., Jr. *Chem. Phys. Lett.* **1993**, *204*, 481–485.
- (15) Morton, J. R.; Preston, K. F. *Chem. Phys. Lett.* **1996**, *255*, 15–18.
- (16) Keizer, P. N.; Morton, J. R.; Preston, K. F.; Krusic, P. J. *J. Chem. Soc., Perkin Trans. 2* **1993**, *6*, 1041.
- (17) Cremonini, M. A.; Lunazzi, L.; Placucci, G. *J. Org. Chem.* **1993**, *58*, 4735–4738.
- (18) Carey, F. A. *Organic Chemistry*, 3rd ed.; McGraw-Hill: New York, 1996.
- (19) Tumanski, B. L.; Bashilov, V. V.; Bubnov, N. N.; Solodnikov, S. P.; Sokolov, V. I. *Russ. Chem. Bull.* **1992**, *41*, 1519.
- (20) Goudsmit, G. H.; Paul, H. *Chem. Phys. Lett.* **1993**, *208*, 73–78.
- (21) Kawai, A.; Okutsu, T.; Obi, K. *J. Phys. Chem.* **1991**, *95*, 9130–9134.
- (22) Kajii, Y.; Nakagawa, T.; Suzuki, S.; Achiba, Y.; Obi, K.; Hibuya, K. *Chem. Phys. Lett.* **1991**, *181*, 100–104.
- (23) Walbinder, M.; Fischer, H. *J. Phys. Chem.* **1993**, *97*, 4880–4881.